Energy Conversion and Management 133 (2017) 20–30

Contents lists available at ScienceDirect

Energy Conversion and Management

journal homepage: www.elsevier.com/locate/enconman

Long term performance degradation analysis and optimization of anode supported solid oxide fuel cell stacks

Tarannom Parhizkar, Ramin Roshandel *

Department of Energy Engineering, Sharif University of Technology, Tehran, Iran

A R T I C L E I N F O

Article history:
Received 9 August 2016
Received in revised form 14 November 2016
Accepted 18 November 2016

Keywords:
Degradation based optimization
Cost of electricity
Optimum operating conditions
Solid oxide fuel cell

A B S T R A C T

The main objective of this work is minimizing the cost of electricity of solid oxide fuel cell stacks by decelerating degradation mechanisms rate in long term operation for stationary power generation applications. The degradation mechanisms in solid oxide fuel cells are caused by microstructural changes, reactions between lanthanum strontium manganite and electrolyte, poisoning by chromium, carburization on nickel particles, formation of nickel sulfide, nickel coarsening, nickel oxidation, loss of conductivity and crack formation in the electrolyte. The rate of degradation mechanisms depends on the cell operating conditions (cell voltage and fuel utilization). In this study, the degradation based optimization framework is developed which determines optimum operating conditions to achieve a minimum cost of electricity. To show the effectiveness of the developed framework, optimization results are compared with the case that system operates at its design point. Results illustrate optimum operating conditions decrease the cost of electricity by 7.12%. The performed study indicates that degradation based optimization is a beneficial concept for long term performance degradation analysis of energy conversion systems.

© 2016 Elsevier Ltd. All rights reserved.

1. Introduction

In recent years, the interest in electrochemical power generation devices based on solid electrolytes has dramatically grown. This concern is due to the advantages of solid electrolytes over liquid electrolytes. For instance, solids can operate in a wider range and therefore, have a lower activation loss [1]. However, the long term operation with respect to contaminants and degradation mechanisms is still mitigates a broad implementation of SOFCs. Thus, a fundamental understanding of degradation mechanisms to analysis the long term operation of SOFCs is of great interest [2].

1.1. Concept

In long term operation, solid oxide fuel cell characteristics and performance deteriorates dramatically. Operating conditions affect the rate of degradation mechanisms. To study SOFC in long term operation, considering degradation mechanisms is unavoidable [3].

The degradation based optimization (DBO) is an optimization framework that considers system degradation mechanisms in the optimization procedure [4]. The flow diagram of the developed DBO framework for SOFC stacks is presented in Fig. 1. At the initial time, system characteristics are known. In the degradation model, the rate of degradation can be calculated based on the system operating conditions. Degradation mechanisms caused by physical, chemical or electrochemical reactions. These mechanisms affect the components characteristics such as the length of triple phase boundaries (TPB) and the electrolyte conductivity. Based on the values of degraded parameters, the system input/output (I/O) performance model calculates system performance indexes (such as system efficiency or output power). At the next time step, updated values are applied to the degradation model and this cycle is repeated until the end of the system operation lifetime. Up to this stage, the system performance deterioration as a function of operating conditions can be presented. At the next step, using this function, the optimum decision variables including operating conditions will be derived.

Generally, optimization models tries to find the operating conditions or/and design parameters which minimize the cost of electricity (COE), maximize the efficiency or profit through system operating lifetime [7]. In this study, our developed DBO framework optimizes operating conditions to achieve a minimum cost of electricity. The DBO framework addresses the influences of a given operating condition on the degradation rate of the system and includes degradation effects in the techno-economic optimization [5].

---

* Corresponding author.

E-mail addresses: Parhizkar@energy.sharif.edu (T. Parhizkar), Roshandel@sharif.edu (R. Roshandel).

http://dx.doi.org/10.1016/j.enconman.2016.11.045
0196-8904/© 2016 Elsevier Ltd. All rights reserved.

Nomenclature

A	area, m^2
c	gas phase concentration, mol m^{-3}
C_{NG}	natural gas cost, \$ m^{-3}
D	mass diffusivity, m^2 s^{-1}
E	activation energy, kJ mol^{-1}
F	Faraday's constant, C $equiv^{-1}$
H	enthalpy, J mol^{-1}
i	current density, A m^{-2}
I	working current, A
k'	constant coefficient
k_{ox}	rate constant for oxidation reaction, m^3 kg^{-1} s^{-1}
$k_{s,cap}$	Nickel particles growth rate
L	length, m
m_{NG}	natural gas mass flow rate, m^3 s^{-1}
M	molecular weight, kg mol^{-1}
n	equivalent electron per mole of reactant, equiv mol^{-1}
ni	number of nickel particles, mol
p	pressure, Pa
P	dimensionless pressure
pr	site occupation probability
R	universal gas constant, J mol^{-1} K^{-1}
r	Nickel particles radius
r_{ox}	rate of oxidation, mol kg^{-1} s^{-1}
S^0	standard entropy, J mol^{-1} K^{-1}
t	time
T	temperature, K
TPB	triple phase boundary, m m^{-3}
u	decision variable
V	voltage, V
x	state variable
X	molar fraction of component in the mixture
β	Ohmic resistance, Ω
η	over potential, V
σ	electrical conductivity, $\Omega^{-1}.m^{-1}$
φ	porosity
ψ	tortuosity
v	diffusion volume of simple molecules, cm^3
α	fraction of the reaction heat that is generated at the anode
δ	pre-exponential factor, Ω^{-1} m^{-2}
θ	overlap angle, 15^0
θ_0	bulk oxygen coverage, dimensionless
γ	exponential activity parameter, kJ mol^{-1}
τ	perimeter

Subscript and super script

0	initial condition
1	bipolar plate (interconnect)
2	fuel channel
3	anode
4	electrolyte
5	cathode
6	air channel
act	activation
c	critical
ch	channel
conc	concentration
eff	effective
f	fuel
max	maximum value
min	minimum value
ocv	open circuit voltage
ohm	Ohmic
opt	optimal
ox	oxydation
ref	reference
x	x direction
y	y direction
z	z direction

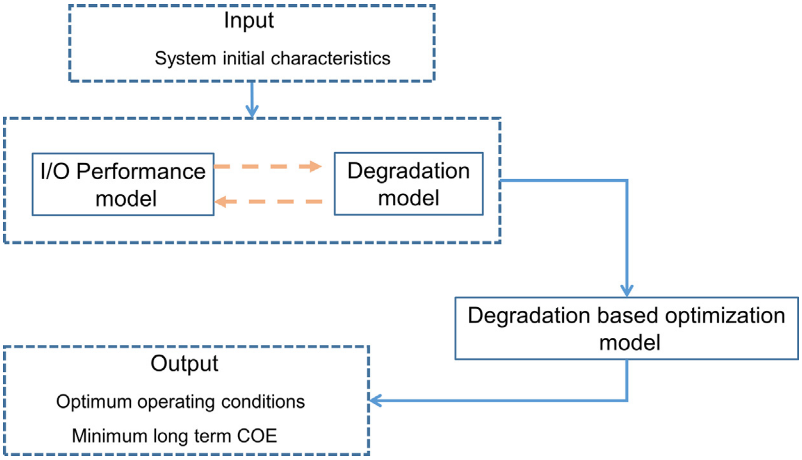
Input
System initial characteristics
I/O Performance model
Degradation model
Degradation based optimization model
Output
Optimum operating conditions
Minimum long term COE

Fig. 1. Proposed framework for considering degradation mechanisms in optimization model.

1.2. Background

The relatively high investment cost of SOFC stacks leads most studies to provide an analysis of possible scenarios that make SOFC applications feasible from an economic point of view [8]. In this respect, recent studies aim at improving the understanding of degradation in SOFC stacks to manage system degradation rate in order to develop cost-competitive SOFC stacks applications in long term operation. The degradation is the process of systems performance deterioration; results from irreversible and gradual growth of damage that happens during systems' life cycle [9]. Degradation models are data driven or developed based on physical, chemical and electrochemical principals (principal based models) [10].

Nakajo et al. [11] presented a data driven model to investigate the effect of different operating conditions on the life time operation of a SOFC stack. The developed model considers main degradation mechanisms includes the reduction of electrolyte ionic conductivity, metallic interconnect corrosion, anode nickel particles coarsening and cathode chromium contamination. The results show that lower stack temperature extends the life time of the stack.

Liu [12] developed a principle based model to provide the distribution of thermal stresses during thermal cycling of a SOFC. The main contribution of the proposed model is to predict the life time of a sample cell. The results show that the current density and cell temperature are the most critical parameters that affect the SOFC microstructure.

A data driven model based on neural networks is developed by Marra [13]. The electrolyte degradation is considered as the main degradation mechanism, and voltage reduction is then presented to highlight the cell deterioration.

In a paper written by Nakajo et al. [14], a data driven model is presented to evaluate the probability of failure (PF) of a SOFC. The electrolyte degradation, metallic interconnect corrosion, anode nickel particle growth and chromium contamination of the cathode are the main degradation mechanisms which are considered in their model. Results show that adjustments of operating conditions, such as flow rates, temperatures, system specific power and methane conversion fraction in the reformer. These parameters decrease the failure probability of anode and cathode by a factor of around 300 and 30, respectively.

The overall resistance model of a SOFC is developed by Aguilar et al. [15]. The sulfur poisoning is considered as the main degradation mechanism. Impedance measurements show that the overall cell resistance can be reduced by diminishing the H_2S content of the entering fuel.

As can be concluded, the data driven models are more commonly applied to analyze the degradation mechanisms. However, in principle based models, the effect of operating conditions on the rate of degradation mechanisms can be well determined [10]. Moreover, the principal based models can be integrated in optimization frameworks which is the main outcome of this study.

Many studies on SOFC stacks optimization have been done in the last decade [6,16]. Mostly the objective of the optimization is maximizing system profit or minimizing system cost regarding design or operating parameters as the decision variables [6]. Based on the reviewed researches, the approximation of system degradation is a well-developed field and a large stream of research are conducted with various purposes. Similarly, operation optimization frameworks regardless considering components degradation are also available. However, obviously, there are not much literatures that combining these two fields.

In this work, the SOFC system operating conditions are optimized regarding degradation mechanisms based on our developed DBO framework. The objective of present study is to minimize the COE of the SOFC stack through its operating life time. The key outcomes resulting from the proposed DBO framework are the stack optimum operating voltage and fuel utilization which lead SOFC stack to operate at the minimum COE over its lifetime.

This paper is organized as follows: in Section 1, the evolution of the SOFC degradation and optimization models are presented. In Section 2, the main degradation mechanisms are introduced and degradation model and I/O performance model of the SOFC are presented. Section 3 presents the optimization framework and the solution approach. Results are presented in Section 4 and finally the study is concluded with an overall discussion on DBO framework in Section 5.

2. Modeling approach

The general operating principle of a SOFC involves the transportation of oxygen from air at the cathode side to the anode side via O^{2-} ions. At the anode side hydrogen is oxidized to form water and release electrons as shown in the reaction (a). The released electrons flow through the external circuit to the cathode side in order to produce electricity and simultaneously react with the oxygen to produce O^{2-} ions as represented in the reaction (b). It should be mentioned that hydrogen is generated by an internal reforming process which takes place at the anode side.

$$H_2 + O^{2-} \rightarrow H_2O + 2e^- \quad (\textit{anode}) \tag{a}$$

$$O_2 + 4e^- \rightarrow 2O^{2-} \quad (\textit{cathode}) \tag{b}$$

The studied SOFC stack is 150 kW with the stationary application. The developed I/O performance model consists of six control volumes: the solid bipolar plate interconnects, the fuel channels, the anode layer, the electrolyte layer, the cathode layer, and the oxidant channels. The properties and constant values used in the simulations are referred to the Wen et al. [6] research.

The main degradation mechanisms of SOFC stacks and the proposed degradation model of studied SOFC is presented in the following sections.

2.1. Degradation mechanisms

During operation, SOFC stacks degrade in many different ways. A number of degradation pathways have been identified that can be categorized based on the occurrence part in the stack as presented in Fig. 2 [17].

2.1.1. Degradation mechanisms in the interconnections

- Oxide layer Formation

The high reactivity of the Zirconium oxide towards La and Sr, apparent at the interface between Lanthanum strontium manganite (LSM) and yttrium stabilized zirconia (YSZ), is the basis of the formation of $La_2Zr_2O_7$ or $SrZrO_3$. Oxidized structure deteriorates the catalytic activity of the cathode. The key parameter which controls the tendency towards the formation of foreign phases is the composition of LSM, and in particular, the amount of Sr. Manganite with a manganese oxide excess is proven to be more stable which is used in the most SOFCs [18].

2.1.2. Degradation mechanisms in the cathode

- Structure changes

Operating at high temperature range of 900–1000 °C may change the microstructural properties. This destruction diminishes triple phase boundary (TPB) and hinders reactants diffusion [19].

- Reaction with chromium

In order to decrease the degradation of interconnecting plates at high operating temperature, plates are coated by a certain quantity of chromium. The input hot air flows on the surface of the metal and causes the transfer of volatile chromium oxide and hydroxide from the surface to the cathode. This mechanism will decrease the TPB length at the cathode side mostly in the cathode supported SOFCs [19].

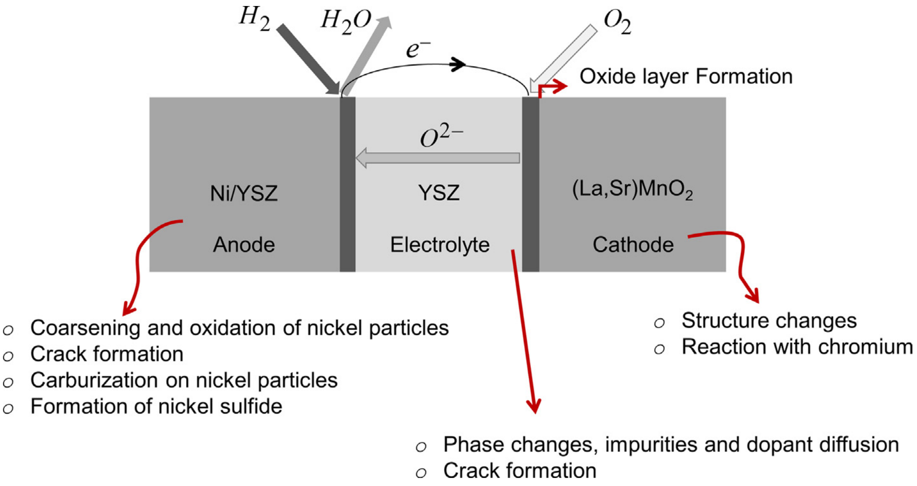

Fig. 2. SOFC degradation mechanisms.

2.1.3. Degradation mechanisms in the electrolyte

- Phase changes, impurities and dopant diffusion

During the system operation at a hazard condition, phase change and impurities diffusion will happen in the electrolyte layer which can decrease the ionic conductivity [18].

- Crack formation

System leakage or mishandled on/off cycles cause the penetration of the undesirable oxygen to the anode side. The existence of the oxygen at the anode side can lead to oxidation of the nickel particles. As there is a considerable difference in the molar volume of Ni and its oxide, this degradation mechanism leads to the formation of internal stress. The internal stress causes tension in the electrolyte layer and crack formation. The permeation of gasses through the crack decreases system performance and accelerates other degradation mechanisms [18].

2.1.4. Degradation mechanisms in the anode

- Coarsening and oxidation of nickel particles

The nickel phase in the yttrium stabilized zirconia (YSZ) structure will be reformed under unsuitable operating conditions. Nickel particle size increases in this undesired reformation mechanism. Moreover, nickel will be oxidized in the presence of oxygen, water, and oxygen ions at the anode side. The increase in the nickel particle size and nickel oxidation, diminishes the contact within the Ni phase. Therefore, electronic conductivity and triple phase boundary will be diminished [20].

- Crack formation

As mentioned before, the oxidation of nickel can cause crack formation in the anode layer [18].

- Carburization on nickel particles

During the internal reforming, hydrocarbons react with steam to form a synthesis gas containing carbon monoxide (CO) and hydrogen (H_2). Then, the steam reacts with the carbon monoxide of the synthesis gas to form carbon dioxide (CO_2) and more hydrogen. This blend is rich in both (CO_2) and (H_2). In this mechanism carbon is deposited on the catalyst layer and as a result reforming process and electrochemical activity will decrease [21].

- Formation of nickel sulfide

The presence of sulfur in hydrocarbon fuels leads to the formation of Ni sulfide. This mechanism decreases the activity in the anodic catalyst [15].

The SOFC performance deterioration caused by all of these different contributions. However, as can be concluded, in actual operating conditions with pure fuel, the main degradation mechanism in anode supported SOFC stacks with Ni-YSZ and monolayer LSM cathode is nickel coarsening and oxidation which is considered in the present paper.

2.2. Governing equations

In this section, a principle based degradation model is developed. As system works, nickel coarsening and oxidation occur which lead TPB and ionic conductivity deterioration. Different researchers used image treatment and analysis to study nickel coarsening mechanism. However, particle coarsening can follow the charging capacitor law which is suggested by Tanasini et al. [22].

$$r_{(t)} = (r^{\max} - r^0)[1 - \exp(-k_{s,cap}t)] + r^0 \tag{1}$$

where r^0 and $r^{\max}$ are the initial and maximum radius of particles and $k_{s,cap}$ is the rate of growth. In many studies the rate of growth is constant and it is derived by fitting to the experimental data at a desired operating conditions. In our study, the rate of growth is a function of temperature that is derived by fitting the experimental data in literature [22].

The second degradation mechanism which is considered in this study is nickel oxidation at anode layer. The main related reactions are presented in Fig. 3.

As can be seen, nickel oxidation can occur via two different pathways. The first pathway is based on pure chemical reactions [23]. In this pathway, nickel can be oxidized in the presence of oxygen or water vapor at anode side as reactions (c) and (d).

$$\mathrm{Ni} + \frac{1}{2}\mathrm{O_2} \leftrightarrow \mathrm{NiO} \tag{c}$$

$$\mathrm{Ni} + \mathrm{H_2O} \leftrightarrow \mathrm{NiO} + \mathrm{H_2} \tag{d}$$

The second reaction pathway is the electrochemical oxidation of nickel which is taking place at the surface between ion conductor and metallic nickel [23]. The oxidation reaction is as reaction (e).

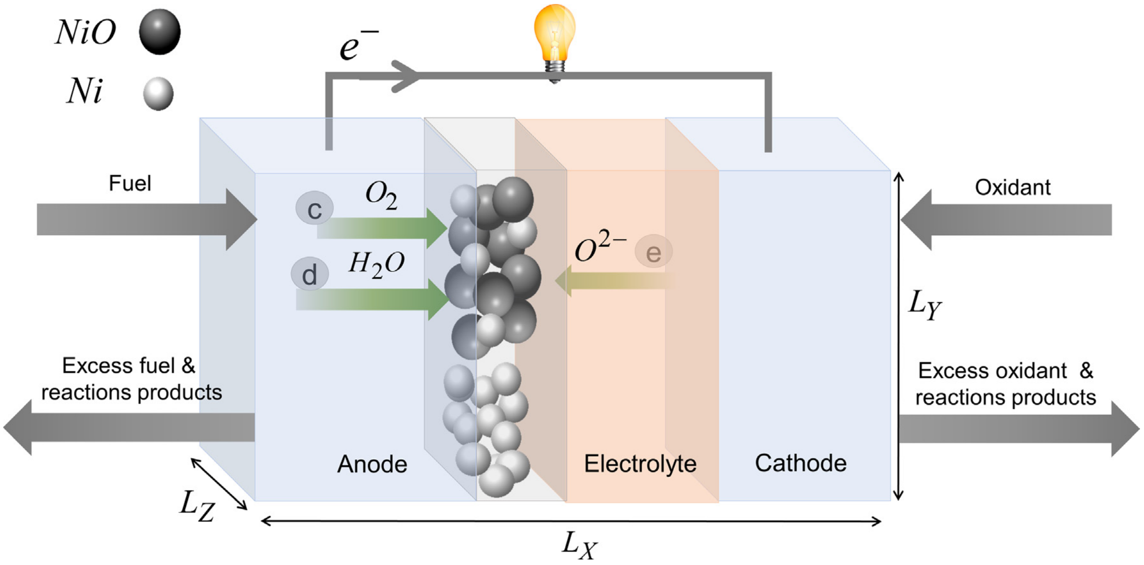
NiO
Ni
e−
Fuel
c
O2
d
H2O
O2−
e
Oxidant
LY
Excess fuel & reactions products
Excess oxidant & reactions products
Anode
Electrolyte
Cathode
LZ
LX

Fig. 3. Main degradation mechanisms of Ni oxidation.

$$Ni + O^{2-} \leftrightarrow NiO + 2e^- \tag{e}$$

In all reactions, the nickel oxidation rate can be calculated as Eq. (2).

$$r_{ox} = k_{ox} c (1 - \theta_O)^2 \tag{2}$$

k_{ox} is the constant rate of reactions which is calculated as Eq. (3).

$$k_{ox} = k' \exp\left(-\frac{E_{ox}}{RT}\right) \exp\left(-\frac{\gamma}{RT}\theta_O\right) \tag{3}$$

Moreover, c is the mole fraction of O_2, H_2O and O^{2-} at anode side that should be defined. The amount of H_2O and O^{2-} depend on input fuel and oxidant flowrates. However, oxygen can exist at the anode side because of leakage or water electrolysis as reaction (f) [24,25].

$$H_2O + H_2 + \frac{1}{2}O_2 \tag{f}$$

The oxygen partial pressure of this reaction can be calculated from Eq. (4).

$$\log (p_{O_2})_{H_2-H_2O} = 2\log\left(\frac{p_{H_2O}}{p_{H_2}}\right) - \frac{26,000}{T} + 5.94 \tag{4}$$

Nickel coarsening and oxidation reduce electrical conductivity and triple phase boundary [26]. The TPB length is calculated as Eq. (5).

$$TPB(t) = 2[(\pi - 2\theta) r(t)]\tau_{Ni}(T) \tag{5}$$

$r(t)$ is the nickel radius which is degraded due to nickel coarsening. In addition, following equation is used to evaluate the perimeter of nickel, τ_{Ni}, as a function of the number of sites in a cluster and the site occupation probability [26].

$$\tau_{Ni}(t) = ni(t)\left(\frac{1 - pr(t)}{pr(t)}\right) + 3.6 ni(t)^{0.5} \tag{6}$$

pr is the site occupation probability which is calculated as Eq. (7) [26].

$$pr(t) = \exp\left[\frac{\ln\left(\frac{\sigma_{eff}(t)}{\sigma_0 \tan\theta}\right)}{1.3}\right] + pr_c \tag{7}$$

Furthermore, the degraded surface also reduces electrical conductivity. The electrical conductivity as a function of site occupation probability is as Eq. (8) [26].

$$\sigma_{eff}(t) = \sigma_0(\tan\theta)[pr(t) - pr_c]^{1.3} \tag{8}$$

As discussed, TPB and electrical conductivity are two parameters which are degraded through time. TPB affects activation and concentration over potentials at anode side. In addition, electrical conductivity increases ohmic over potential at anode side. The effects of TPB and electrical conductivity reduction on over potentials can be calculated by applying degraded values of TPB and electrical conductivity to the SOFC I/O performance model. The governing equations of system I/O performance model which leads to power generation calculation are presented in Table 1, [27].

3. Optimization procedure

The optimization objective is to minimize the cost of electricity (COE) through system lifetime regarding degradation mechanisms. The objective function is presented as follow, whereas satisfying constraints related to the system.

$$Max J[u(t), x(t)] = \frac{Investment\ cost + Fuel\ cost + Maintenance\ cost}{Power\ generation} \tag{27}$$

The investment cost is the cost of SOFC stack and fuel cost is the cost of consumed natural gas during given operating lifetime as Eq. (28).

$$Fuel\ cost = \int_t^{t+T} (m_{NG}(t) \times C_{NG}) \cdot dt \tag{28}$$

The maintenance/replacement cost represents the replacement cost of a stack cell in a given operating conditions. In most studies, total maintenance/replacement cost is considered as a constant value. However, in this study, system maintenance cost is corresponding to the rate of a degradation mechanism. In this way, system actual operating cost can be calculated continuously. The maintenance cost is calculated as Eq. (29).

$$Maintenance\ cost = \int_t^{t+T} \left(\frac{dni(t)}{dt} \times replacement\ cost\right) \cdot dt \tag{29}$$

Table 1
SOFC I/O performance model governing equations.

Output voltage		
Actual operating voltage	$V(t) = V_{OCV} - \left(\sum_j \eta_{ohm,j}(t) + \eta_{conc,3}(t) + \eta_{conc,5} + \eta_{act,3}(t) + \eta_{act,5}\right), \quad j = 1,3,4,5$	(9)
Open circuit voltage	$V_{OCV} = \frac{-\left(H_{H_2O} - H_{H_2} - \frac{1}{2}H_{O_2}\right) + T \times \left(S^0_{H_2O} - S^0_{H_2} - \frac{1}{2}S^0_{O_2}\right) - RT\ln\left[\frac{P_{H_2O}}{P_{H_2}(P_{O_2})^{0.5}}\right]}{2F}$	(10)
Ohmic over potential		
Ohmic over potential in regions 1, 4	$\eta_{ohm,j} = I\beta_j, \quad j = 1,4$	(11)
Electrical resistances of interconnect and electrolyte	$\beta_1 = \frac{L_1}{L_y L_z \sigma_1} + \frac{L_2}{(1+n_{ch})L_t L_y \sigma_1} + \frac{L_6}{(1+n_{ch})L_t L_z \sigma_1}$	(12)
	$\beta_4 = \frac{L_4}{L_y L_z \sigma_4}$	(13)
Ohmic over potential in regions 3, 5	$\eta_{ohm,j}(t) = \frac{I(A_{j,opt}(t) - L_y L_z)L_{j,opt}(t)}{2A_{j,opt}(t)L_y L_z(1-\emptyset_j)\sigma_4} + \frac{I(L_j - L_{j,opt}(t))}{L_y L_z(1-1.8\emptyset_j)\sigma_i(t)}, \quad j = 3,5$	(14)
Area of active TPB regions	$A_{j,opt}(t) = (1 + 2L_{j,opt}(t)/D_{p,j})L_{yz}$	(15)
Average diameter of electrodes parallel pores	$D_{P,j} = D_{W,j}\emptyset_j/(1-\emptyset_j)$	(16)
Concentration over potential		
Concentration over potentials at cathode	$\eta_{conc,5} = \frac{RT}{4F}\ln\left(\frac{P_{O_2}}{P_{O_2,TPB}}\right)$	(17)
Concentration over potentials at anode	$\eta_{conc,3}(t) = \frac{RT}{4F}\ln\left(\frac{P_{H_2}P_{H_2O,TPB}(t)}{P_{H_2O,TPB}(t)P_{H_2O}}\right)$	(18)
Water partial pressure	$P_{H_2O,TPB}(t) = p_f X_{H_2O} + \frac{RT\psi_3}{2FD_3(t)\emptyset_3}\frac{L_3 I}{L_y L_z}$	(19)
Hydrogen partial pressure	$P_{H_2,TPB}(t) = p_f X_{H_2} - \frac{RT\psi_3}{2FD_3(t)\emptyset_3}\frac{L_3 I}{L_y L_z}$	(20)
Oxygen partial pressure	$P_{O_2,TBP} = p_{air} - (p_{air} - X_{O_2}p_{air})\exp\left(\frac{RT\psi_5 L_5 I}{4FD_5\emptyset_5 p_{air}L_y L_z}\right)$	(21)
Diffusivities in anode and cathode	$D_3 = \frac{1.43\times10^{-7}T^{1.75}(M_{H_2}+M_{H_2O})^{0.5}}{p_f(2M_{H_2}M_{H_2O})^{0.5}\left(v^{\frac{1}{3}}_{H_2} + v^{\frac{1}{3}}_{H_2O}\right)^2}$	(22)
	$D_5 = \frac{1.43\times10^{-7}T^{1.75}(M_{O_2}+M_{N_2})^{0.5}}{p_{air}(2M_{O_2}M_{N_2})^{0.5}\left(v^{\frac{1}{3}}_{O_2} + v^{\frac{1}{3}}_{N_2}\right)^2}$	(23)
Activation over potential		
Activation over potentials	$\eta_{act,j}(t) = \frac{RT}{\alpha nF} sinh^{-1}\left(\frac{i}{i_{0,j}(t)}\right), \quad j = 3,5$	(24)
Exchange current densities	$i_{0,j}(t) = \gamma_a TPB(t)\left(\frac{P_{H_2}}{P_{ref}}\right)\left(\frac{P_{H_2O}}{P_{ref}}\right)\exp\left(-\frac{E_j}{RT}\right), \quad j = 3,5$	(25)
Output power density		
SOFC output power density	$power(t) = V(t) \times i$	(26)

$\frac{dni(t)}{dt}$ is the rate of nickel degradation and *replacement cost* is the cost of a cell replacement because of nickel degradation.Power generation term in the objective function is the generated power through system operating lifetime which is presented as Eq. (30)

$$Power\ generation = \int_t^{t+T} Power(t) \cdot dt \tag{30}$$

$$Power(t) = V(t) \times i \times A(t) \tag{31}$$

$V(t)$ and $A(t)$ are actual operating potential and active surface area over time. The optimization procedure is also subject to several constraints. It is assumed that SOFC is designed to work at a specific temperature and current density ranges. The proposed constraints are expressed in Eqs. (32) and (33).

$$T^{\min} \leqslant T \leqslant T^{\max} \tag{32}$$

$$i^{\min} \leqslant i \leqslant i^{\max} \tag{33}$$

Moreover, it is assumed that the SOFC stack works until half of nickel particles in electrode is degraded [30]. In this case SOFC stack fails and cell should be replaced.

$$ni(t) \geqslant \frac{ni^0}{2} \tag{34}$$

Finally, the initial condition of oxidized surface area is equal to zero as Eq. (35).

$$\theta_O = 0 \tag{35}$$

To solve the optimization problem, evolutionary techniques can be used to find the optimum decision variables due to their versatility and ability to optimize complex systems [30]. In particular, the proposed optimization model has many local optima solutions with nonlinear objective function. Moreover, its parameters changes over time. Genetic algorithm (GA) technique appears to be a promising algorithm for handling this kind of optimization problems.

GA algorithm has a parallel-population based search with stochastic selection of many individual solutions, stochastic crossover and mutation that can lead model to the optimal solution in a short time. The GA algorithm initializes a population with random candidate solutions. Each candidate solution is called a ‘population’ which determines a vector of operating conditions. GA algorithm evaluate the objective function of the population and take its information into account to generate a new set of operating conditions. The population moves through the solution space following some basic formulae in search of a global optimum. After several generations, only the ‘most optimum’ one can transmit information onto others, making the optimization very fast in comparison to other evolutionary techniques [31].

4. Results and discussion

To evaluate the performance, effectiveness and efficiency of the DBO framework of SOFC stacks, it is applied to a 150 kW Ni-YSZ anode supported SOFC with a stationary application. The physical properties utilized to obtain simulation results are referred to Wen et al. [6] research.

4.1. Model validations

To validate the I/O performance model, a comparison between model outputs and results published by Wen et al. [6] is undertaken. The comparison illustrates that under the same SOFC geometric dimensions and operating conditions, the modeling output accuracy is compelling enough to validate the numerical simulation. Furthermore, the voltage degradation rate at different current densities and fuel utilizations are used to validate the component degradation model. The results show that the model prediction agrees with the experimental data gathered by Muller et al. [32] and the results are nearly close.

4.2. System characteristic

Fig. 4 presents the V-I curves, at start and 10,000 h of system operation at three different temperature ranges. As it appears, the temperature affects the shape of the power profile. By increasing the temperature, the maximum power value moves to the right of the graph indicating the higher current density. Operation at high temperature range also results in low activation loss, which leads system to operate at a higher level of power and voltage. On the other hand, the degradation rate is found to increase with higher temperature. It is worth noticing that high temperature ranges, which correspond to higher voltage and output power, lead to an acceleration of the degradation and result in higher voltage and output power deterioration rates. In other words, in order to reach higher output power in long term operation, power deterioration rate dependency of temperature should be taken into consideration.

Fig. 4(c) shows that the voltage is degraded about 12% after 10,000 h of operating at a high temperature range (1108 K). The breakdown of SOFC overpotentials after 10,000 h of operation is presented in Fig. 5.

As can be seen in the figure, the activation overpotential which originates from irreversibilities of electrochemical reactions has the greatest portion of overpotentials.

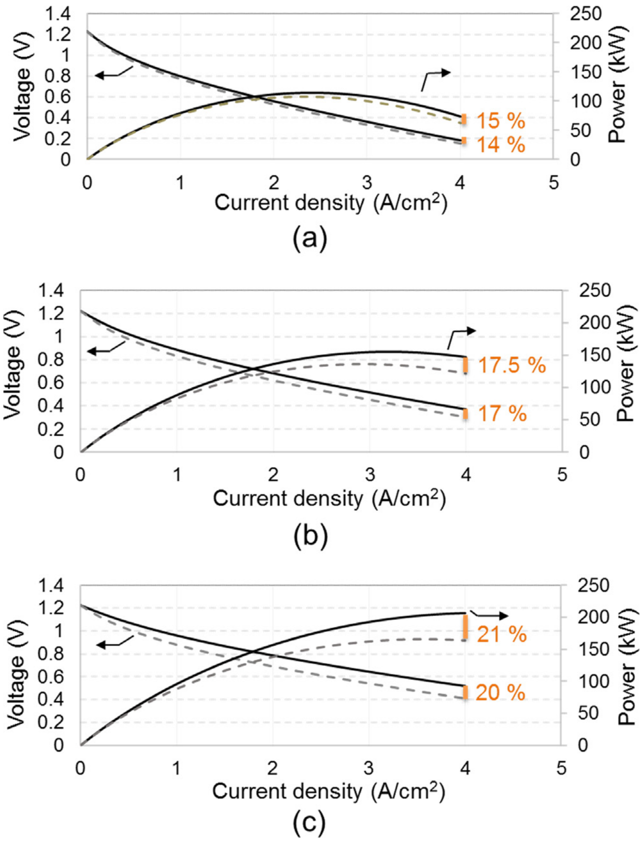

Fig. 4. Polarization and power curves at start (—) and after 10,000 h (- - -) for (a) low-1048 K (b) medium-1078 K (c) high-1108 K temperatures.

In contrast, the concentration overpotential that is generated by mass transport in electrodes, is often neglected due to the high gas diffusion rate at high operating temperatures. Therefore, as is shown, it has the least value [33]. The last overpotential is the ohmic over potential which is generated by the ionic and electronic charge transfer resistances. The ohmic resistance is important in all types of cells and is essentially linearly proportional to the current density. For an anode supported SOFC, the ohmic loss is smaller than in the other types of SOFC cells [33]. Results indicate that around 28% of the total over potential is due to the ohmic loss.

Each overpotential is caused by system inevitable physical, chemical and electrochemical losses (actual losses) and losses which are added to the overpotentials because of system degradation mechanisms (degradation losses).

Fig. 5 depicts the proportion of these losses on each overpotential. For instance, a quarter of the activation loss occurs as a result of degradation mechanisms. The TPB is the most important parameter which affects the activation overpotential. The TPB length is mainly affected by the microstructure of the electrodes. Nickel coarsening and oxidation decreases TPB length drastically. Additionally, based on the results, degradation has the most effect on the concentration overpotential, and about 45% of the concentration overpotential is due to the anode degradation. That is because of the fact that nickel degradation mechanism changes the structure of materials and decreases diffusivity dramatically. Furthermore, at a high temperature level the electrical conductivity of nickel oxide and nickel particles are nearly the same. Consequently, the effect of nickel degradation on ohmic loss is negligible.

4.3. System degradation

In this section, the outputs of the degradation model are reported. All the results are obtained under the similar geometrical features and the same operating conditions reported in Section 4.2 (47% fuel utilization at three different temperature ranges). Fig. 6 (a) depicts the behavior of the active surface area over time. While the system is working, nickel coarsening and oxidation occur. The increase in the nickel particle size and nickel oxidation, decrease the contact within the Ni phase and, therefore, the active surface area is diminished. As nickel coarsening and oxidation rates are accelerated at upper temperature ranges, the deterioration of active surface area would be higher.

Fig. 6(b) indicates output power over time. This figure shows that the output power decreases through time as a consequence of TPB and anode layer conductivity reduction. Furthermore, after a while, the power value becomes constant, depending on the operating temperature. In addition, as can be seen, at upper temperature ranges, the initial output power of SOFC is higher, but the deterioration rate is accelerated as well and power falls drastically through time. On the contrary, at lower operating temperatures, the system operates at a lower power level with a smooth deterioration rate over time.

4.4. System productivity and cost of electricity (COE)

As discussed in Section 4.3, operating conditions have a great impact on the system power generation and efficiency in a long term operation. In this section a voltage and fuel utilization sensitivity analysis for system productivity and cost of electricity is performed. In Table 2, the economic assumptions applied to the COE calculations are summarized.

The influence of the cell voltage on power generation through system lifetime and cost of electricity is shown in Fig. 7(a). The productivity reaches its maximum value at 0.51 V and the system generates 5856 kW h power through its operating lifetime. It

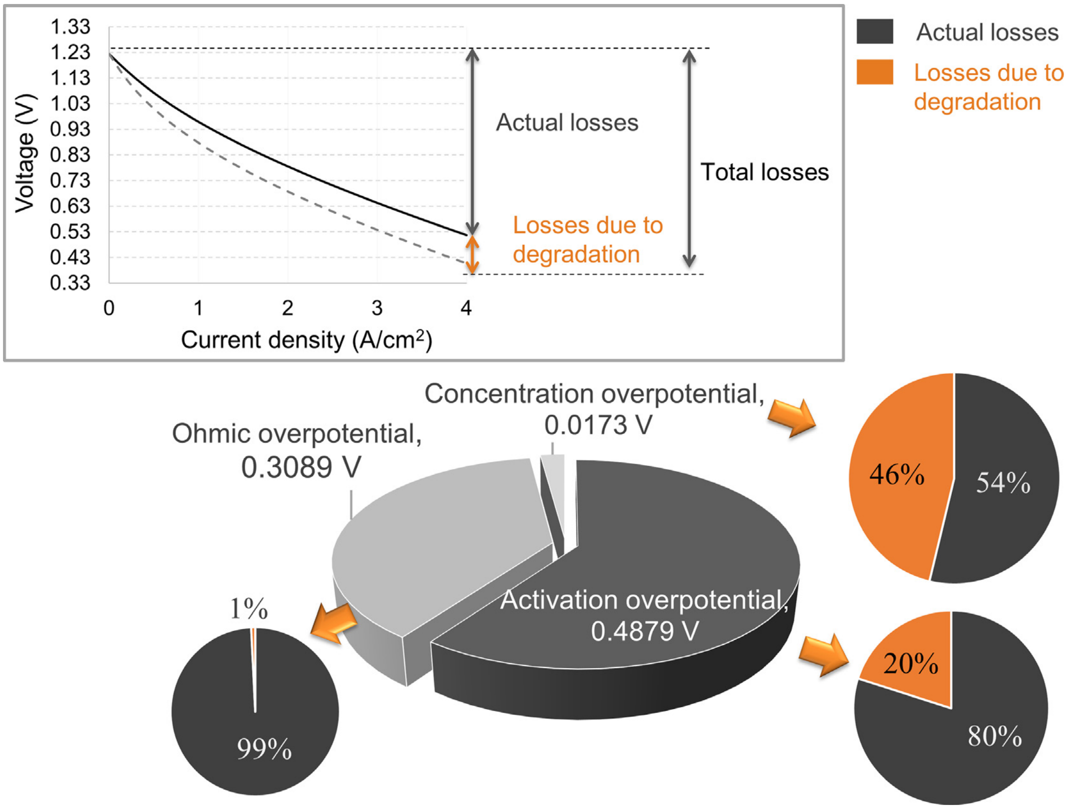

Fig. 5. Degradation based and actual losses after 10,000 h operating at (1108 K, 4 A/cm^2).

should be noted that the COE shows its minimum value at the same voltage. At low cell voltages, output power is low, and it causes power generation to be at its minimum level. As cell voltage increases, system operates at upper power levels and the power generation increases till it reaches its peak. By increasing the cell voltage, the degradation rate is accelerated, therefore, system operating lifetime decreases and system performance deteriorates more rapidly. This lead system to have a lower productivity (power generation over the system lifetime).

Moreover, the sensitivity of COE is illustrated in Fig. 7(a) as well. At low cell voltage the electrical plant efficiency is low. As a consequence, a large natural gas stream is consumed, which is a cost dominant factor. Moreover, as mentioned, at low voltage, the productivity is low. High fuel cost and low productivity increases COE at low voltages. At higher voltage ranges, the system becomes more efficient and generates more power until the COE reaches its minimum value. At higher cell voltages, system overall efficiency deteriorates drastically, therefore, fuel cost increases and, as before mentioned, system productivity decreases. These facts cause an upward trend in the COE.

In Fig. 7(b), the sensitivity analysis of fuel utilization is illustrated. Fuel utilization is related to the natural gas feed stream. As fuel utilization increases, system power density rises and, as a result, system productivity increases up to 3000 kW h, provided when fuel utilization is adjusted to about 60%. At higher fuel utilization ranges, system operates at upper power densities but the degradation mechanism rate increases and performance deteriorates more rapidly as well, thus productivity drops.

Fuel utilization variation has the same effect on COE trend as voltage variation. Increasing fuel utilization, enhances system efficiency and productivity until system reaches its minimum COE value. At higher fuel utilization, performance and efficiency deteriorate drastically because of the higher degradation rates and this leads system to have a higher fuel cost with lower productivity. These two effects cause system to operate at higher COE.

4.5. System optimization

As already discussed, SOFC operating conditions have a great impact on system productivity and COE. The optimum operating conditions which lead system to have a minimum COE are determined according to the proposed degradation based optimization (DBO) model. To study the advantages of the DBO model, two optimization strategies are compared. In the first strategy, system operating conditions are optimized to maximize power density regardless of degradation mechanisms. Usually, these operating conditions are defined by the manufacturer of the system and here in it is based on Wen et al. [6] optimization results (base case). In the second strategy, system operates at the conditions which are derived from our proposed DBO model. The derived optimum operating conditions are presented in Table 3.

Fig. 8(a) presents the predicted COE of the system at mentioned operating strategies (Table 3). As can be seen, operating under the DBO strategy, decreases system COE up to 7.12%. Under the base case strategy, the system operates at a higher power level, but degradation mechanisms are not controlled and performance deteriorates drastically. Moreover, uncontrolled degradation mechanisms, cause system to fail earlier, therefore, the power generation decreases. On the other hand, the DBO strategy, considers degradation mechanisms. This leads system to operate at a lower power level over a longer operational lifetime, therefore, system COE would be lower. The breakdown of the system lifetime COE for both operating strategies is illustrated in Fig. 8(b). This figure indicates that the proposed DBO strategy leads to a more efficient and durable operation of SOFC stacks. At the DBO strategy, the power deterioration rate is much lower than in the base case

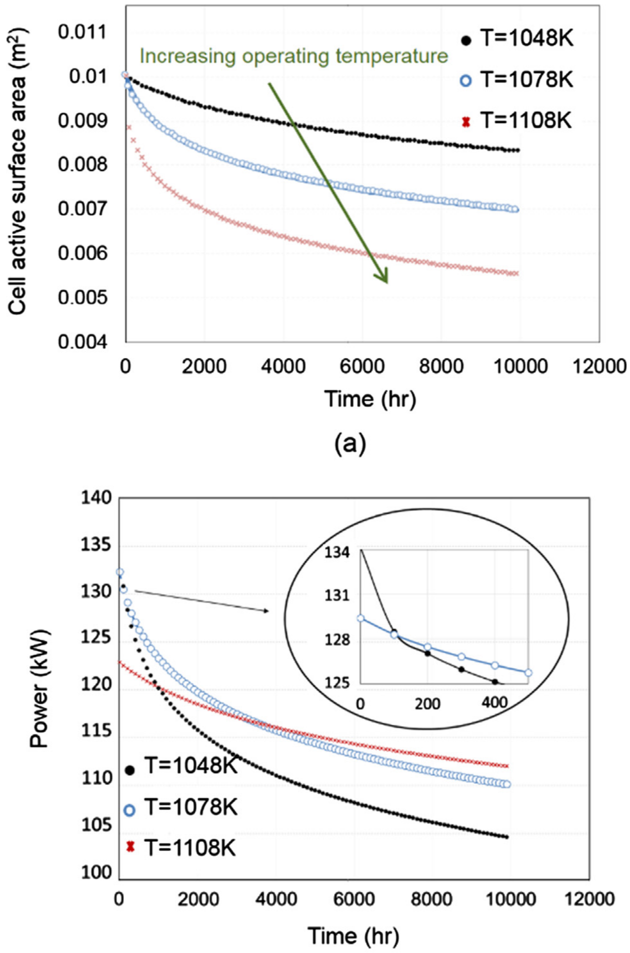

(a)

(b)

Fig. 6. Cell active surface area and output power over time at three temperatures.

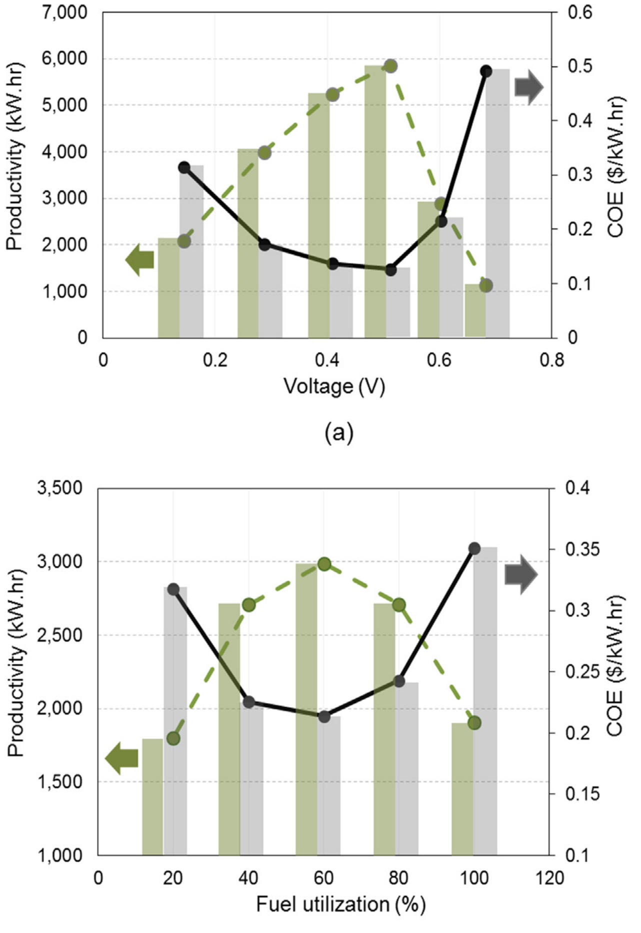

(a)

(b)

Fig. 7. Voltage and fuel utilization sensitivity analysis of COE and productivity.

Table 2
Assumed economic parameters.

Parameter	Value	Reference year
Investment cost	$1620\,\$\,\mathrm{m}^{-2}$	[28]
Interest rate	10%	–
Fuel cost	$0.03\,\$\,\mathrm{kW\,h}^{-1}$	[28]
SOFC Single cell cost	$90\,\$\,\mathrm{kW}^{-1}$	[29]

Table 3
Optimum operating conditions resulting from DBO.

	Value	Unit
Fuel utilization	40	%
Voltage	0.60	V
Cell temperature	1033	K

and system operating lifetime is longer. As a result, system generates more power. It should be noted that most of the SOFC lifetime cost is in the initial investment of the system, which is the same for both operating strategies. Furthermore, although power generation is lower in the base case, the fuel cost is higher in comparison with the DBO strategy. The main reason is that the long term efficiency in the base case is much lower than in the DBO due to the accelerating degradation rates.

4.6. The economic parameters' effect on the optimum COE

The contributors to the system cost are the investment of the SOFC stack, the maintenance/replacement and the fuel cost. The notable fraction of the total cost is in the investment. Consequently, the primary focus of the total cost reduction should be centered on SOFC stacks. In recent years, new materials and high manufacturing technology have sharply reduced the SOFC price and The Fuel Cells and Hydrogen Joint Undertaking (FCH JU) has predicted that the stack cost is projected to be $2000\,\$/\mathrm{kW}$ by 2020 [34]. In addition, the fuel cost variation can have different effects on the COE. The sensitivity of the COE to the reduction of investment cost to $2000\,\$/\mathrm{kW}$ and the fuel cost fluctuation of ±20% is performed in this section. The results illustrate that system economics could be improved by decreasing fuel and investment cost. However, COE is less sensitive to fuel cost compared to investment cost because the main portion of the system cost is in the initial investment.

At the current fuel cost, decreasing system capital cost by half could potentially reduce the COE by around 30%, and the SOFC system cost of electricity can be more competitive with the grid. In addition, when the investment cost is lower, the impact of the fuel cost on COE will be greater. For instance, 4% COE reduction is obtained by a 20% reduction in fuel cost at the current investment cost. However, by cutting the investment cost in half and reducing fuel cost by about 20%, the COE could decrease up to 6%.

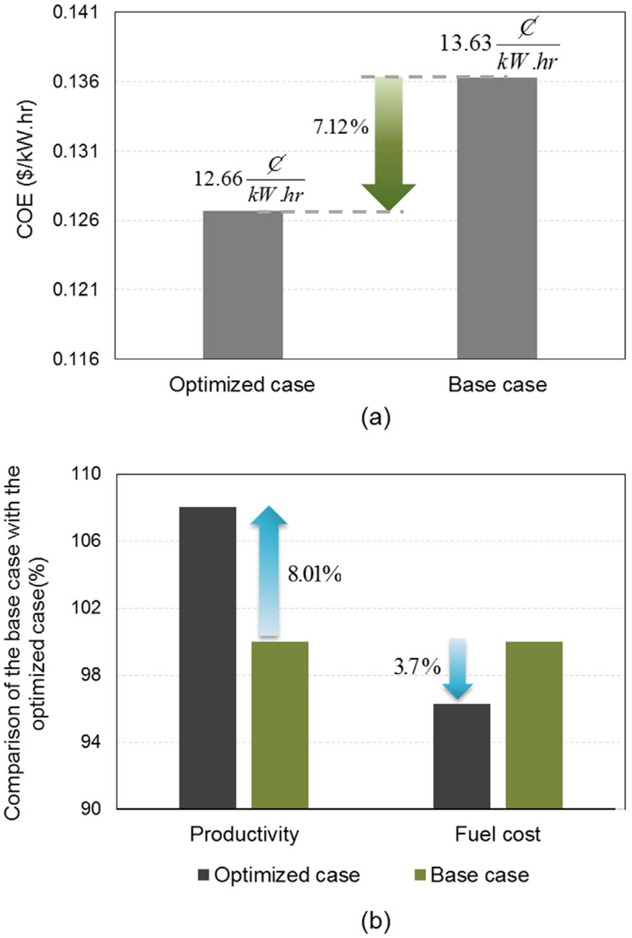

Fig. 8. Comparison of COE, productivity and fuel cost for optimum and base case conditions.

5. Conclusion

This research aims to contribute to the field of degradation based optimization methodology. The proposed model optimizes operating conditions of an anode supported SOFC system regarding degradation mechanisms to achieve minimum cost of electricity in long term operation. Based on the suggested degradation model, the influence of different operating conditions on anode side degradation and its effect on performance deterioration is illustrated. Moreover, the effect of operating conditions on power generation and cost of electricity is also determined and the optimum operating conditions to achieve minimum COE are derived. To show the effectiveness of the proposed framework, results are compared with the optimum base case strategy which its operating conditions are optimized regardless of degradation mechanisms. Results show that using the DBO framework, system COE is 7.12% lower in comparison with the base case. Moreover, the sensitivity analysis of COE indicates that the COE is less affected by fuel cost than investment cost.

In this study, the validation and demonstration of the degradation based optimization model laid the framework for considering degradation in long term performance analysis of SOFCs. However, this framework can be expanded to any other energy systems including power plants, and refineries.

References

[1] Ho ThX. Dynamic characteristics of solid oxide fuel cell with direct internal reforming of methane. Energy Convers Manage 2016;113–1:44–51. doi: http://dx.doi.org/10.1016/j.enconman.2016.01.049.

[2] Baldinelli A, Barelli L, Bidini G, Di Michele A, Vivani R. SOFC direct fuelling with high-methane gases: optimal strategies for fuel dilution and upgrade to avoid quick degradation. Energy Convers Manage 2016;124:492–503. doi: http://dx.doi.org/10.1016/j.enconman.2016.07.051.

[3] Barelli L, Bidini G, Cinti G, Ottaviano A. SOFC regulation at constant temperature: experimental test and data regression study. Energy Convers Manage 1 June 2016;117:289–96. doi: http://dx.doi.org/10.1016/j.enconman.2016.03.028. ISSN 0196-8904.

[4] Roshandel Ramin, Parhizkar Tarannom. Degradation based optimization framework for long term applications of energy systems, case study: solid oxide fuel cell stacks. Energy 15 July 2016;107:172–81. doi: http://dx.doi.org/10.1016/j.energy.2016.04.007. ISSN 0360-5442.

[5] Shafie-khah M, Moghaddam MP, Sheikh-el-eslami MK, Catalao JPS. Optimised performance of a plug-in electric vehicle aggregator in energy and reserve markets. Energy Convers Manage 2015;97:393–408. doi: http://dx.doi.org/10.1016/j.enconman.2015.03.074.

[6] Wen H, Ordonez JC, Vargas JVC. Single solid oxide fuel cell modeling and optimization. J Power Sources 2011;196-18:7519–32. doi: http://dx.doi.org/10.1016/j.jpowsour.2010.10.113.

[7] Caliandro P, Tock L, Ensinas AV, Marechal F. Thermo-economic optimization of a Solid Oxide Fuel Cell – Gas turbine system fuelled with gasified lignocellulosic biomass. Energy Convers Manage 2014;85-1:764–73. doi: http://dx.doi.org/10.1016/j.enconman.2014.02.009.

[8] Joneydi Shariatzadeh O, Refahi AH, Rahmani M, Abolhassani SS. Economic optimisation and thermodynamic modelling of SOFC tri-generation system fed by biogas. Energy Convers Manage 15 November 2015;105:772–81. doi: http://dx.doi.org/10.1016/j.enconman.2015.08.026. ISSN 0196-8904.

[9] Bogdanoff JL, Kozin F. Probabilistic models of cumulative damage. 1st ed. New York: Wiley-Interscience; 1985. doi: http://dx.doi.org/10.1002/qre.4680010413.

[10] Bae SJ. Degradation models, Technical Report No.123, School of Industrial & Systems Engineering. Atlanta, Georgia, U.S.A.: Georgia Institute of Technology; 2010.

[11] Nakajo A, Mueller F, Brouwer J, Vanherle J, Favrat D. Progressive activation of degradation processes in solid oxide fuel cells stacks: part I: lifetime extension by optimisation of the operating conditions. J Power Sources 2012;216-15:449–63. doi: http://dx.doi.org/10.1016/j.jpowsour.2012.05.078.

[12] Liu L. Solid oxide fuel cell reliability and performance modeling and fabrication by spray pyrolysis, PhD thesis, Iowa State University, Ames, Iowa, 2011. <http://lib.dr.iastate.edu/cgi/viewcontent.cgi?article=1446&context=etd>.

[13] Marra D. Development of solid oxide fuel cell stack models for monitoring, diagnosis and control applications PhD thesis. Salerno, Italy: University of Salerno; 2012. http://elea.unisa.it:8080/jspui/bitstream/10556/1014/Ellipsis/tesi%20D.%20Marra.pdf.

[14] Nakajo A, Mueller F, Brouwer J, Vanherle J, Favrat D. Mechanical reliability and durability of sofc stacks. part I: modelling of the effect of operating conditions and design alternatives on the reliability. Int J Hydrogen Energy 2012;37–11:9249–68. doi: http://dx.doi.org/10.1016/j.ijhydene.2012.03.043.

[15] Aguilar L, Zha Sh, Cheng Zh, Winnick J, Liu M. A solid oxide fuel cell operating on hydrogen sulfide (H_2S) and sulfur-containing fuels. J Power Sources 2004;135-1:17–24. doi: http://dx.doi.org/10.1016/j.jpowsour.2004.03.061.

[16] Shariatzadeh OJ, Refahi AH, Abolhassani SS. Economic optimisation and thermodynamic modelling of SOFC tri-generation system fed by biogas. Energy Convers Manage 2015;105-15:772–81. doi: http://dx.doi.org/10.1016/j.enconman.2015.08.026.

[17] Faes A, Hessler-Wyser A, Presvytes D, Vayenas CG, Van herle J. Nickel-Zirconia anode degradation and triple phase boundary quantification from microstructural analysis. Fuel Cells 2009;9-6:841–51.

[18] Nakajo A. Thermo mechanical and Electrochemical Degradation in anode-supported solid oxide fuel cell stacks. Phd Dissertation, Industrial Energy Laboratory, In Science And Technology Engineering, Epa University, France; 2011.

[19] Nakajo A, Mueller F, Brouwer J, Van herle J, Favrat D. Progressive activation of degradation processes in solid oxide fuel cell stacks: part II: Spatial distribution of the degradation. J Power Sources 2012;216:434–48.

[20] Von V. Nickel oxidation in solid oxide cells: modeling and simulation of multi-phase electrochemistry and multi-scale transport. Phd Dissertation, Energy Technology department, Process Engineering and Biological Stuttgart University; 2013.

[21] Marina OA, Coyle CA, Thomsen EC, Edwards DJ, Coffey GW, Pederson LR. Degradation mechanisms of SOFC anodes in coal gas containing phosphorus. Solid State Ionics 2010;181:430–40.

[22] Tanasini P, Cannarozzo M, Costamagna P, Faes A, VanHerle J, Hessler-Wyser A, et al. Experimental and theoretical investigation of degradation mechanisms by particle coarsening in sofc electrodes. Fuel Cells 2009;09–5:740–52.

[23] Neidhardt JP. Nickel oxidation in solid oxide cells: modeling and simulation of multi-phase electrochemistry and multi-scale transport. PhD. Dissertation, University of Stuttgart, Germany. <http://elib.uni-stuttgart.de/opus/Ellipsis/Neidhardt_Nickel_oxidation_in_SOC.pdf>; 2013.

[24] Nehter P. A high fuel utilizing solid oxide fuel cell cycle with regard to the formation of nickel oxide and power density. J Power Sources 2007;164–1:252–9. doi: http://dx.doi.org/10.1016/j.jpowsour.2006.08.037.

[25] Monnerat B, Kiwi-Minsker L, Renken A. Mathematical modelling of the unsteady-state oxidation of nickel gauze catalysts. Chem Eng Sci 2003;58–21:4911–9. doi: http://dx.doi.org/10.1016/j.ces.2002.11.006.

[26] Hardjo DM, Karan K. Numerical modeling of nickel-impregnated porous YSZ-supported anodes and comparison to conventional composite Ni-YSZ electrodes. ECS Trans 2011;35–1:1823–32. doi: http://dx.doi.org/10.1149/1.3570171.

[27] Huang K, Goodenough JB. Solid oxide fuel cell technology principles performance and operations. 1st ed. Woodhead Publishing; 2009.

[28] Trendewicz AA, Braun RJ. Techno-economic analysis of solid oxide fuel cell-based combined heat and power systems for biogas utilization at wastewater treatment facilities. J Power Sources 2013;233-1:380–93.

[29] Weimar M, Chick L, Gotthold D, Whyatt G. Cost study for manufacturing of solid oxide fuel cell power systems. U.S. Department of Energy, Report No.: PNNL-22732; 2013.

[30] Changrong H, Chen T, Wang WG. The mechanical and electrical properties of Ni/YSZ anode support for solid oxide fuel cells in Anodes. China: Ningbo Institute of Material Technology and Engineering; 2008.

[31] Elsied Moataz, Oukaour Amrane, Youssef Tarek, Gualous Hamid, Mohammed Osama. An advanced real time energy management system for microgrids. Energy 1 November 2016;114:742–52. doi: http://dx.doi.org/10.1016/j.energy.2016.08.048. ISSN 0360-5442.

[32] Muller A, Weber A, Beie HJ, Krugel A, Gerthsen D, Tiffee E. Influence of current density and fuel utilization on the degradation of the anode. In: Proc. of the 3rd European Solide Oxide Fuel Cell Forum, Nantes France; 1998.

[33] Yang Sh, Chen T, Wang Y, Peng Z, Guo Wang W. Electrochemical analysis of an anode-supported SOFC. Int J Electrochem Sci 2013;8:2330–44.

[34] http://www.fch.europa.eu; 2015.